

A study on the feasibility of optical OFDM modulation for V2X communication.

Hugo RIMLINGER¹ and Jose A. LAZARO²

¹*Institut des Sciences Appliquées de Lyon, 20 avenue Albert Einstein
69621 Villeurbanne cedex, France*

²*Universitat Politècnica de Catalunya, Jordi Girona 31, 08034, Barcelona, Spain.*

Abstract— In this paper, we will show that vehicle to everything (V2X) communication are possible in the optical domain instead of traditional radio frequency. For that, we elaborate a communication system using real values Orthogonal Frequency Division Multiplexing (OFDM) modulation for Intensity Modulated Direct Detection (IM/DD). We implemented this system accordingly to Wi-Fi 802.11p physical layer requirements. We also implemented Low Density Parity Check (LDPC) encoding for error corrections. In this report, we will give an overview on transmitting and receiving functions. We will also discuss about the applicability of our communication system for V2X, based on a performance metric called Error Vector Magnitude (EVM).

Keywords: optical OFDM, IM/DD, V2X, 802.11p, LDPC encoding, EVM.

I. INTRODUCTION

IN last decades, major development in vehicles were made possible by using electronics. Indeed, the ability to perform V2X communication, thanks to the introduction of new devices (sensors, antennas, processors, etc...) has changed our vision on conceiving vehicles. Nowadays, the number of equipment connected to wireless networks (cellular, Wi-Fi) is slightly increasing with the development of connected vehicles and its applications. To support these devices, constructors and operators are seeking for new techniques to enhance vehicular access network environment (VANET). In this project, we studied on the feasibility of performing V2X communications in the optical domain using Intensity Modulated Direct Detection (IM/DD) devices. In this type of equipment, optical signal is directly modulated by the intensity of the radio frequency (RF) signal.

Because the generation and reception are direct (light intensity converted into electrical signal at the receiver and inversely at the transmitter), the optical signal generated is modulated in amplitude. Therefore, the RF signal produced must be real (phase or frequency modulation are not available). Because V2X -and mobile devices in general- relies on using Orthogonal Frequency Division Multiplexing (OFDM)

modulation, we implemented a variant of this modulation that produce a real signal (optical OFDM). Using optical domain is valuable for V2X communication because they do not interfere with traditional RF signals. This allows to open a brand-new spectrum to perform V2X communications. Also, as we will see, the cost of optical devices (laser, photodetector) are suitable for industry application. Because we still need to produce a RF signal before conversion in the optical domain, we chose to implement the physical structure of 802.11p, a Wi-Fi standard specially designed for V2X applications.

The structure for this paper is the following: In part II, we will give you an overview on use-cases and requirements of V2X and motivate our choice of implementing 802.11p standard. In part III we will explain main functions of our transmitter system: modulation, encoding and conversion from electrical to optical domain. In part V we will focus on explaining how to counter channel's effects and perform timing synchronization between transmitter and receiver. Finally, in part VI, we present our result and discuss about the effectiveness of such a communication system for V2X.

II. V2X COMMUNICATIONS PERFORMANCES AND 802.11P STANDARD.

In this section, we will identify the need for V2X communications depending on the scenario of use. We will also present briefly the IEEE 802.11p and LTE-V2X release, which has already been validated by 3GPP for V2XC application.

A. Use-cases and requirements of V2X communications.

V2X wireless communications englobe many different use-cases such as traffic efficiency, collision warning or vehicles coordination. To achieve these applications, vehicles need to receive and send information about their environment and state. Because these messages imply safety issues, these communications must fulfil strict requirements in terms of latency and reliability. Below are summarize the different scenarios of V2XC [11]:

Cooperative sensing and awareness.

This application englobes a large range of use-cases like the distance between two vehicles, detection of an intersection or light signalization. Messages broadcasted to the other devices

implied in the V2X communication environment (vehicles, cells, sensor, etc...) in a short and medium range.

Vulnerable road user.

In this case, communications are effectuated between a vehicle and user's smartphone (if the user doesn't have one this application relies on the car's camera sensor) and enable the detection of pedestrians near the vehicle.

Cooperative maneuver.

Here, the idea is to exchange information between two vehicles or between a vehicle and an infrastructure to facilitate change of line or intersection crossing. It is a very critical scenario that requires ultra-high reliability (>99%) and very low latency (<3ms).

Traffic efficiency.

With all the information shared between vehicles and infrastructure, V2X communication is aimed to be used to enhance traffic density and traffic rate. These are a type of large range communications which requires less important performance constrain (between 90% and 95% of reliability and 1ms end-to-end latency).

Because safety is the most important aspect of connected vehicles, V2XC's performances are mostly focused on a high data rate (from 5 to 25000 kbps), low end-to-end latency (from 3ms to more than 1s) and an ultra-high reliability (from 90% to above 99%). Of course, because some of these applications are more critical than others (such as the vulnerable road user detection compare to the traffic efficiency) the requirements are not the same, imposing to have a flexible and performing network.

B. 802.11p physical layer requirements.

One of the reasons leading to choose this standard is that it enables Ad-Hoc communications with autonomous resources allocation (center frequency, bandwidth, etc...). This is an important feature for future development in connected vehicles and particularly in out-of-coverage scenarios. Indeed, in this situation, a protocol for direct communication is necessary. In 802.11p, autonomous resource allocation is made possible by Wireless Access Vehicular Environments (WAVE) protocol [10]. Because we were focusing on testing the feasibility of optical communication, we did not implement it. Nevertheless, as we will see, implementing WAVE would be possible using our communication system (see part V.D). Principle requirements of 802.11p physical layer are summarized in table 1 [9].

We based our measurements on frames of 500 bytes, respecting the bandwidth and frame duration (see measurements figure 1. a/1. b). At each frame is associated a preamble of 13 OFDM symbols, used for timing synchronization, channel estimation and frequency offset correction (see part IV).

In figure 1.a, we can clearly see the alternance between preamble and frame. Indeed, before transmission, the short preamble is multiplied by $\sqrt{13/6}$ to normalize the signal power [9]. You may also have noticed that the signal is modulated by

Parameter	Value
Total number of subcarriers	64
Number of data subcarrier	48
Number of pilots	4
Number of guard band	12
Number of short preamble symbols	10
Number of long preamble symbols	2
Carrier spacing (in MHz)	0.1562
Bandwidth available (MHz)	10
Maximum Centre frequency (GHz)	5.85
Maximum Centre frequency (GHz)	5.925

Tab 1: Principal 802.11p physical layer parameters and their value [9].

amplitude, since we are using a variant of OFDM modulation for IM/DD systems (see part III.B).

In next section we will detail the main steps of our transmitter, figure 3 shows the equipment and the experimental set-up we used.

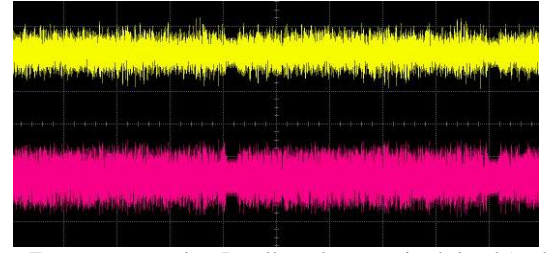


Figure 1.a: Frame representation. In yellow, the transmitted signal (peak to peak voltage equal to 500 mV). In pink the optical received signal (peak to peak voltage equal to 400 mV). Steps of low voltage correspond to the preamble. Frame time measured of 50 ms.

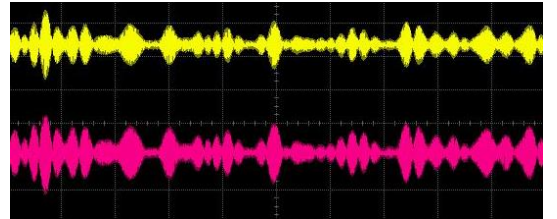


Figure 1.b: As in figure 1.a, yellow correspond to transmitted signal and pink to the received one. We can clearly see that the signal is modulated in Amplitude (optical OFDM).

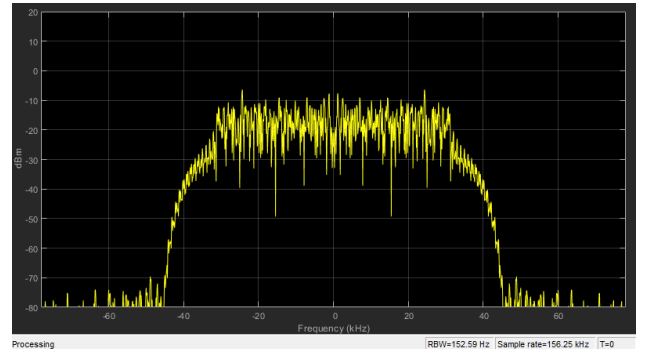


Figure 1.c: Spectrum of the transmitted signal, sample rate of and bandwidth of 85 MHz (including guard band).

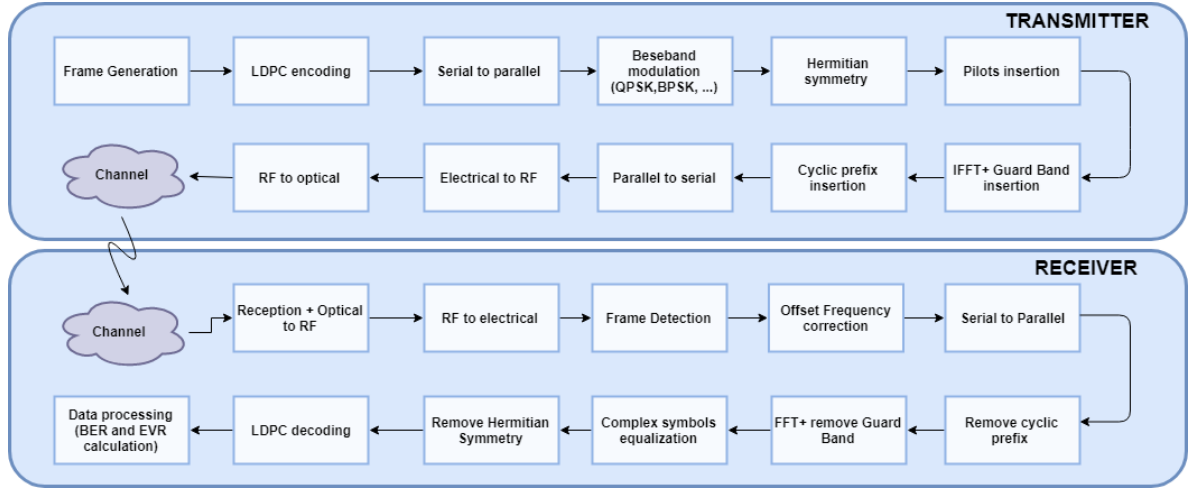


Figure 2: Principal blocks of our communication system (Transmitter and Receiver).

III. OPTICAL TRANSMITTER.

The transmitter is composed in three parts: first, we generate frames prepared for encoding. After that we perform LDPC encoding and optical OFDM modulation. The electrical signal is then converted into Radio frequency domain. Finally, by using an laser, the optical signal is produced by direct intensity modulations, IM, of the laser, and transmitted through the air by two GRIN lenses, coupled to the laser's and detector's fibers (see figure 3).

Next part will be focused on explaining step by step main functions of our transmission system. "*OFDM synchronization*" [15], from MATLAB, has been used as a base for our program. Figure 2 shows the main steps followed by the optical transmitter.

A. Real OFDM modulation and LDPC encoding.

Many optical devices use Intensity Modulated Direct Detection (IM/DD) technique. In this method, based on the utilisation of a laser and photodetector, the electrical RF signal modulates the intensity of the optical signal. IM/DD devices can only modulate the optical signal in amplitude (part III.B).

Therefore, the signal produced in RF domain must be real. For that, Hermitian symmetry is applied to the complex symbols produced after broad band modulation (BPSK, QPSK, 16-QAM, etc...). We also use LDPC encoding, a technique vastly used in digital communication for its high performances (around the Shannon's limit [6]).

LDPC encoding.

LDPC is an encoding method of linear block code. Its name low density parity check comes from the matrix generation which is composed of few numbers of 1. Each line of H corresponds to a code word and respects [5]:

$$x_1 \oplus x_2 \oplus \dots \oplus x_N = 0 \text{ and } H \cdot c^T = 0 \quad (III.1)$$

Where x_i represents each code symbols of a code word c . N is the number of columns in H (size of a code word) and \oplus is the logical 'AND'. We can have two types of low-density parity check: irregular and regular. In regular LDPC matrix, the

Main components of our communication system.

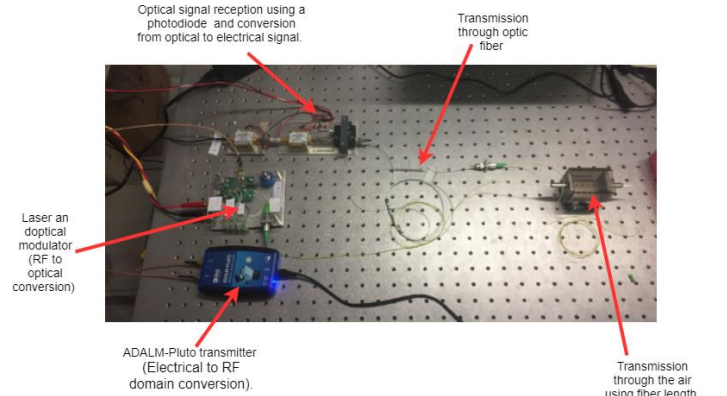


Figure 3: Picture of the main components of the communication system (experimental set-up).

number of '1' in each line is equal and each equation has the same size (irregular LDPC matrix allows to relax these conditions). Nevertheless, decoding follows the same principle for both regular and irregular parity check matrix.

We have two types of decoding for LDPC: soft decoding and hard decoding. For both, it is based on two types of nodes (c-nodes and v-nodes) to detect and correct errors. The number of v-nodes and c-nodes correspond respectively to the number of columns and rows in the matrix H . Each v-nodes is linked to several c-nodes, figure 4 shows how c-nodes and v-nodes are connected. In order to detect and correct an error, each node is going to exchange information iteratively [6]:

1. In this first step, each v-nodes is going to send the received bit to every c-nodes it relates to.
2. After receiving each bit from its v-nodes, a c-nodes is going to send back the value of the bit that, for him, is the best. For that, a c-node is going to determine the value of the bit (for one v-node) to fulfil the parity check (III.1), assuming that the information sent by the other v-nodes is right. This operation is repeated for

every v-nodes connected to the c-nodes and for every c-nodes.

3. Therefore, in this step, v-nodes receive several information (value of bits) corresponding to its number of connections with c-nodes. Then, each v-nodes is going to choose the new correct bit's value by a majority vote. If it receives more '1' than '0', then v-node is going to choose '1' (and inversely).
4. Go to step 2. As we can see, this algorithm does not have an end, therefore, we can determine the maximum number of loops that we want.

After the end of this algorithm, we chose the closest code word corresponding to our decoding (in term of Hamming distance). If two codewords have the same distance of Hamming, one of the two is picked randomly.

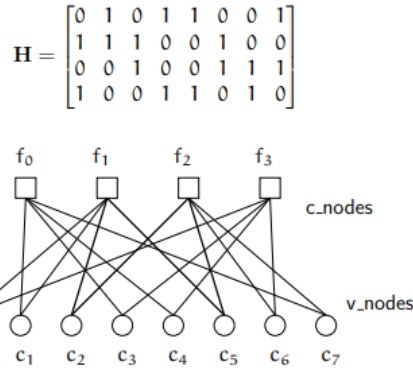


Figure 4: This example from "Advanced Numerical Communication" of INSA de Lyon, shows the correspondence between H and the link between v-nodes and c-nodes. Note that this matrix is too small to be "low density".

Hermitian symmetry. To obtain a real signal after the Invers Fast Fourier Transform (IFFT) algorithm (used for the OFDM modulation), we need the input to be Hermitian symmetric [13]. To be Hermitian symmetric, symbols must fulfil (in the frequency domain):

$$X(m) = X^*(N - m) \quad (III.2)$$

With $0 \leq m \leq \frac{N}{2} - 1$ and N the number of subcarriers. The Hermitian symmetry is an important constrain on the signal and results in a loss of spectrum efficiency (only $\frac{N}{2} - 1$ subcarriers of the OFDM symbols carry unique data). In fact, only 23 subcarriers available to carry payload data:

$$N_{Data} = FFTLength - N_{Hermi} - N_{Pilots} - 2 = 23 \quad (III.3)$$

After applying Hermitian symmetry, pilots are added to the signal for future equalization (respecting Hermitian symmetry). Pilots are generated with a Pseudorandom Noise (PN) sequence which are less sensible to the noise (see part V. C). After that,

IFFT is used to generate OFDM symbols and cyclic prefix is added. Finally, the OFDM signal is passed from serial to parallel.

Conversion from electrical to RF domain

This conversion is performed by the ADALM-Pluto Software Defined Radio (SDR), which is a relatively simple device to use. Indeed, this equipment has been especially made for engineering students, as an introduction tool for real environments communications. Nevertheless, the performances of ADALM-Pluto radio allow us to cover a large spectrum and, as shown in table 2, it can support important sample rate. Also, its price is reasonable for industrial applications (around 171

Parameter	Value
Minimum centre Frequency (MHz)	70
Maximum centre Frequency (GHz)	6.0
Minimum sample rate (kHz)	520
Maximum Sample rate (MHz)	61.44
MATLAB compatibility	yes
Python compatibility	yes
Transmission and Reception of RF signals	yes

Tab 2: ADALM-Pluto SDR capabilities [18].

euros).

B. Conversion from RF signal to optical domain with IM.

To produce the optical signal, the RF electrical single is used for feeding a laser, therefore the laser is directly modulated by the RF signal. Nevertheless, a good linear conversion is required. Figure 5 shows how this conversion is performed by the used laser. Horizontal axis represents the biasing current that is added to the RF signal. Indeed, because we are working with light, we can only transmit positive amplitude [4].

This biasing current must be chosen wisely. Below a certain threshold (around 12 mA), the laser is emitting non-coherent light and at much lower efficiency. After this threshold, our laser is almost perfectly linear. Nevertheless, for too high values of current (near the limit of 60mA), the signal can be distorted, due to loss of linearity.

We also measure the maximum center frequency handled by the

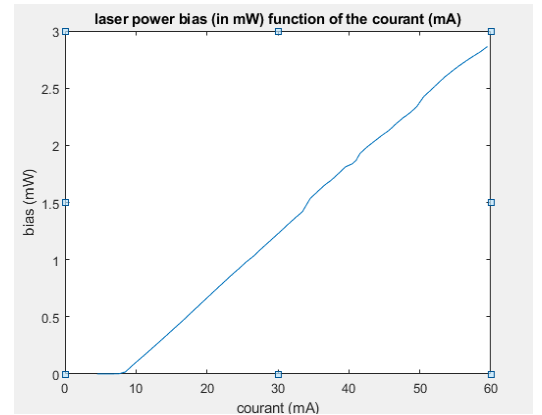


Figure 5: Characterization of the laser output. We measure the output optical power function of the biased courant added to the signal by the laser.

laser around 1GHz, limiting our range of measurements (see part VI. B). Note that, at the receiver, the same detection technique is applied, using a photodiode to measure the

important because with that, we can both perform timing synchronization and phase offset correction. As we mentioned previously, timing synchronization is made by using short

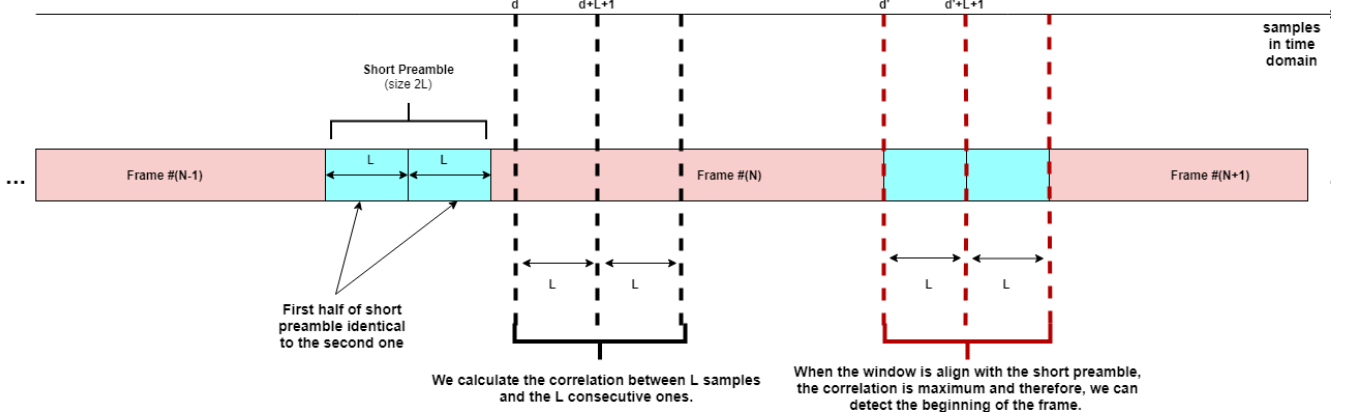


Figure 6: illustration of the frame detection principle. Notice that we used a short preamble composed of only two identical parts for better visualization.

intensity of the optical signal.

IV. OPTICAL RECEIVER.

Because of channel's effect, delay induced by reflections or difference of synchronization between receiver and transmitter's oscillators our signal is highly affected at the receiver. To reconstruct the information, by the receiver functions in three main steps: timing synchronization (frame detection), frequency offset correction, and equalization. In this section, we will detail each of these steps, beginning by the frame detection.

A. Frame Detection, timing synchronization.

As we mentioned previously, phase and frequency offset can impact the OFDM signal, causing ISI. The received signal is of the form:

$$r_r(d) = A(d)e^{-j2\pi f_c t} e^{j2\pi \Delta f t} \quad (IV.1)$$

Where $A(d)$ is the amplitude of the d^{th} symbol f_c the center frequency and $e^{j2\pi \Delta f t}$ the phase offset (Δf is the frequency offset). From this expression, we can notice that this phase offset is the same for the whole OFDM symbol (frequency offset concern only the center frequency). It is especially

preamble, OFDM modulated (figure 7).

As you can see, within each OFDM symbol composing the short preamble, we have a repetition of 4 identical symbols. Based on this periodicity, we calculate the correlation, between L samples and the consecutive L samples, $L = \text{FFTlength} / 4$ (see figure 6) [7]. The correlation, $P(d)$:

$$P(d) = \sum_{m=0}^{L-1} r_r^*(d+m) r_r(d+m+L) \quad (IV.2)$$

is maximum when the window is aligned with one of the symbols within the short preamble, note that this position is not influenced by the phase offset frequency. Nevertheless, the amplitude attained by $P(d)$, because of channel's noise, can vary.

To resolve this problem, Schmid and Cox in [5] propose a time metric of the form:

$$M(d) = \left[\frac{|P(d)|}{R(d)} \right]^2 \quad (IV.3)$$

Where $R(d)$, is the energy of the reference signal:

$$R(d) = \sum_{m=0}^{L-1} |r(d+m+L)|^2 \quad (IV.4)$$

It is used as a normalization factor, reducing the effect of the noise on $P(d)$. Like that, $M(d)$ attain the same amplitude, not being influenced by the noise.

B. Frequency Offset correction.

As OFDM relies on the orthogonality between each of its subcarriers to avoid interference inter symbol, it is sensible to frequency offset. To counter these effects, we used two approaches.

First frequency offset.

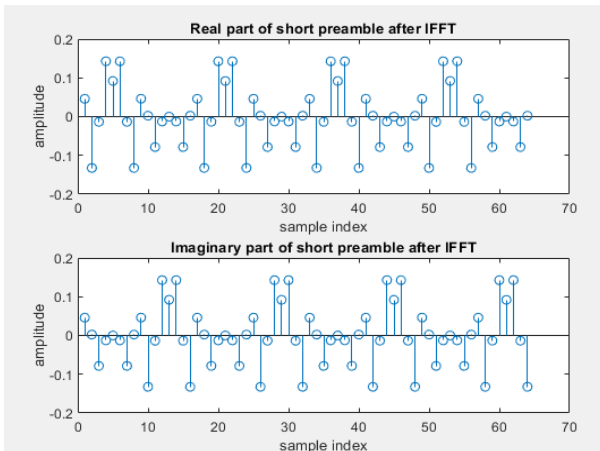


Figure 7: on top: real part of short preamble after IFFT. Below: imaginary part of short preamble after IFFT.

After finding the beginning of the frame, based on the definition of $P(d)$, we make a first estimation of the frequency offset. Indeed, because we have:

$$r_r(k+m) = A(k+m)e^{-j2\pi f_c t} e^{j2\pi \Delta f(k+m)T_e} \quad (IV.5)$$

$$r_r(k+m+L) = A(k+m+L)e^{-j2\pi f_c t} e^{j2\pi \Delta f(k+m+L)T_e} \quad (IV.6)$$

Thus, we obtain:

$$P(k) = e^{j2\pi \Delta f k T_e} \sum_{m=0}^{L-1} r_r^*(k+m) r_r(k+m+L) \quad (IV.7)$$

Notice that, when the window is aligned with one the symbols of the short preamble $r_r^*(k+m) \approx r_r(k+m+L)$. Therefore $P(k)$ is real and we can calculate:

$$\Delta f = \frac{\arg(P(k))}{2\pi L T_e} \quad (IV.8)$$

The frequency offset is then used to resample the received signal at the original center frequency.

Second Frequency offset Correction.

Because $r_r^*(k+m)$ and $r_r(k+m+L)$ are not exactly equal (due to channel's effects), it remains a residual frequency offset that can be corrected by estimating the average sample rate over a certain number of OFDM symbols (20 in our case).

When we finally have corrected the center frequency offset and find the beginning of the frame, we must equalize and demodulate our symbols.

C. Equalization.

As described in part IV, channels change both in-phase and quadrature of complex symbols, as we can see in figure 8. Equalization is made in two parts: a first one using the long preamble and a second one using pilots. Long preamble is used for channel estimation, generated using a PN sequence, like the pilots. It is composed of 53 subcarriers and repeated 2 times in the preamble (see table 1). Long preamble is more effective on data equalization than pilots because it occupies every subcarrier of an OFDM symbol. Also, this first equalization on both data and pilots using long preamble, reduce significantly channel's effects on pilots and allowing a better interpolation and equalization of the data.

Advantage of using a PN sequence.

A pseudo-random noise sequence is a stream of bits, generating pseudo-randomly using a polynomial root. Even if pseudo-random noise sequence is cyclic (the sequence repeat itself over the time), locally, PN sequence possess noise randomness characteristics. This property is useful because, as the noise, PN sequence have very low inter-correlation and high autocorrelation [8]. Therefore, it could be used for time synchronization, generating the same PN sequence at the receiver (using the same polynomial root give the same PN sequence). In our case, it is a way for us to reduce frame detection errors because short preamble has a very low

correlation with long preamble (which could not be the case without using PN sequence). For the equalization, PN sequence are also valuable because, being random, it gives a better estimation of channel's effects on the signal [8]. Thus, we use it for both long preamble and pilots.

Now that we have presented you our communication system, we would like to expose you its performances. For that, we conducted two series of measurements, one function of the center frequency and output gain and the other by attenuating the transmitted signal.

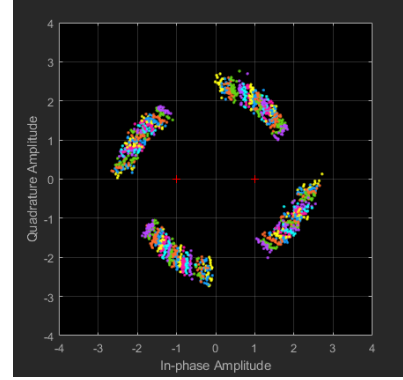


Figure 8.a: Received symbols for QPSK modulation. We can clearly see a rotation (phase offset) and a spreading of the constellation (noise).

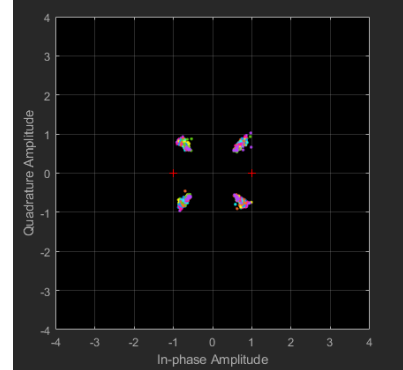


Figure 8.b: QPSK constellation after equalization and phase offset correction.

V. RESULTS AND FUTUR WORKS

A. Metric for Measurements: The Error Vector Magnitude.

Because our Bit Error Rate (BER) was very low during our first measurements (VI.B), we decided to use a more precise metric called Error Vector Magnitude (EVM). Instead of comparing each decoded bit, EVM calculate the difference of power between received and transmitted complex symbols, therefore, this measure must be applied in the frequency domain, just after the FFT.

Because we are going to calculate EVM for different reference constellation (QPSK, BPSK, 16-QAM), having different amplitudes, we need to normalize it for comparison. Normalization mean that the EVM does not depend on the constellation power. EVM is define as the Root Mean Square

(RMS) error between received and reference symbol's amplitude [1][2]:

$$EVM_{RMS} = \left[\frac{\frac{1}{N} \sum_{n=1}^N |S_n - S_{0,n}|^2}{\frac{1}{N} \sum_{n=1}^N |S_{0,n}|^2} \right]^{1/2} \quad (V.1)$$

With S_n the n^{th} normalized symbol's amplitude of the received constellation. MS error is calculated using $S_{0,n}$, the ideal reference symbol normalized amplitude, corresponding to S_n . Because normalization factor for S_n and $S_{0,n}$ are different, we cannot directly translate equation (V.1) into its normalized form.

Normalization factor for reference constellation.

In [1] it is defined the normalization factor of the reference constellation by:

$$A_0 = \frac{N}{\sum_{n=1}^N [(V_{I,0,n})^2 + (V_{Q,0,n})^2]} \quad (V.2)$$

Where $V_{I,0,n}$ and $V_{Q,0,n}$ are respectively the in-phase and quadrature voltage of the ideal constellation of N symbols.

Normalization factor for received constellation.

The same way, [1] defines also a normalization factor for the received constellation, based on the measured power:

$$A = \left[\frac{T}{P_v} \right]^{1/2} \quad (V.3)$$

P_v is the measured power of a constellation of T received symbols and can be approximate as:

$$P_v = \sum_{t=1}^T [(V_{I,t})^2 + (V_{Q,t})^2] \quad (V.4)$$

$V_{I,t}$ and $V_{Q,t}$ represent respectively the in-phase and quadrature voltage of the received constellation.

Using equation (V.2), (V.3) and (V.1), we finally obtain the expression of EVM_{RMS} [1][2]:

$$EVM_{RMS} = \left[\frac{\frac{1}{T} \sum_{t=1}^T |I_t - I_{0,t}|^2 + |Q_t - Q_{0,t}|^2}{\frac{1}{N} \sum_{n=1}^N |I_{0,n}|^2 + |Q_{0,n}|^2} \right]^{1/2} \quad (V.5)$$

With $I_t = V_{I,t}|A$ because we take the inverse of the power to calculate A) is the normalized in-phase amplitude of the t^{th} symbol of a constellation of T symbols. Similarly, $Q_t = V_{Q,t}|A$ is the normalized quadrature amplitude of the t^{th} symbol of the received constellation. These amplitudes are respectively compared with the corresponding t^{th} symbol of the transmitted constellation: $Q_{0,t} = V_{Q,t}|A_0$ and $I_{0,t} = V_{I,t}|A_0$.

Next section shows results on the performances of our communication system using this metric.

B. EVM and BER function of the output gain and center frequency.

In order to test our communication system, we wanted to have an idea on its capabilities through a wireless channel (figure 3). Therefore, we measured both BER and EVM function of the center frequency and output gains at the ADALM-Pluto transmitter. These results are given figure 9.a/9. b / 9. (results for BPSK is given in the appendix) and as you can see, we did not represent the BER because it was always equal to 0 (no error after demodulation and equalization).

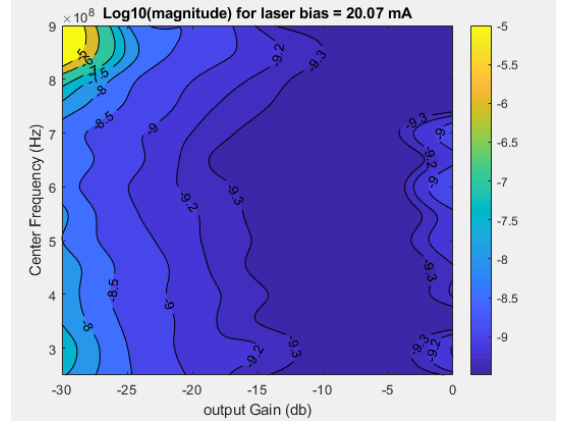


Figure 9.a: evolution of EVM, function of center frequency and output gain. Representation using $10 * \text{Log}_{10}(\text{EVM})$ for QPSK modulation.

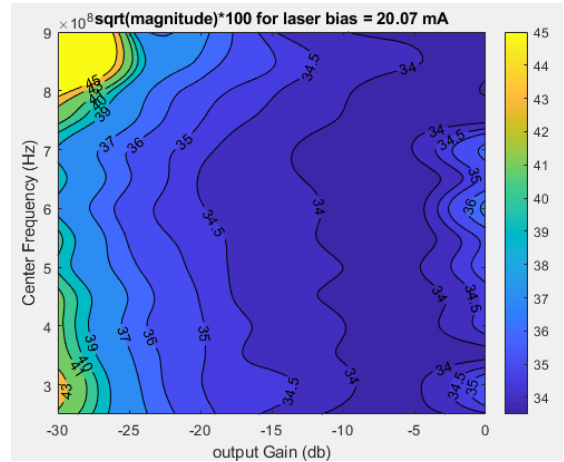


Figure 9.b: evolution of EVM, function of center frequency and output gain. Representation using $\text{sqrt}(\text{EVM}) * 100$ for QPSK modulation (percentage).

We chose to take a range of frequency from 250 MHz to 900 MHz, which correspond to the minimum center frequency of the ADALM-Pluto and maximum frequency supported by our laser (see part III on the equipment). To obtain a reasonable number of samples, we chose a frequency pad of 50 MHz (i.e. 14 center frequencies). To make our measurements reliable to noisy outdoor transmission we varied the output gain from -30dB (in case of very good channel condition, we can lower the output power) to 0 dB (in case of bad channel's conditions).

These results were expected because, as we can see, for a center frequency close to the limit of our system, the EVM is more important. Also, when the output power is very low or too high, this EVM is also higher. Also, we have been able to

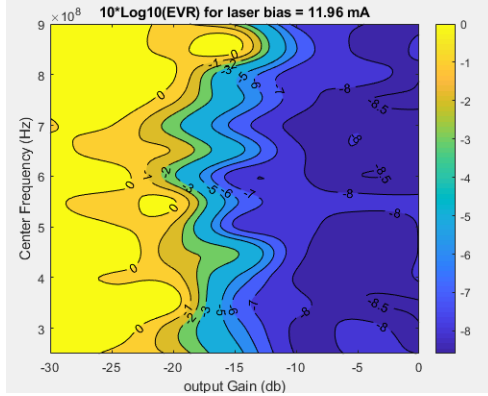


Figure 9.c: evolution of EVM, function of center frequency and output gain. Representation using $10 \cdot \text{Log}_{10}(\text{EVM})$ for 16QAM.

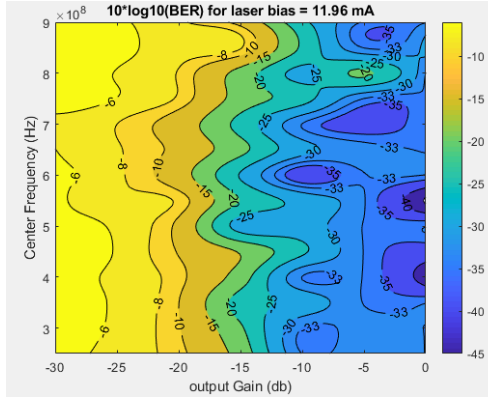


Figure 9.d: evolution of BER, function of center frequency and output gain. Representation using $10 \cdot \text{Log}_{10}(\text{BER})$ for 16QAM.

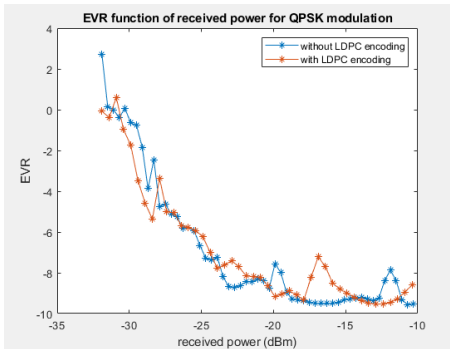


Figure 10.a: evolution of EVM, function the received power, with and without LDPC encoding.

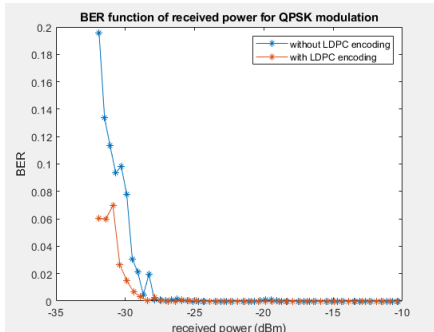


Figure 10.b: evolution of BER, function the received power, with and without LDPC encoding.

perform 16-QAM modulated transmission. As we can see, this modulation is more affected by the noise (higher power constellation) because the BER is non equal to 0. Finally, we can see, that it exists some kind of relation between the EVM (figure 9.c) and the BER (9.d).

As we mentioned previously, we wanted to see if a correlation existed between BER and EVM. For that, we decided to use an optical attenuator that reduce the output power transmitted after the laser (figure 10.c).

C. EVM and BER function of the received power.

Because we wanted our system to be tested in high losses channel's conditions, we also measured BER and EVM when attenuating the signal. For that, we placed an optical attenuator that reduce the received signal power. Figure 10.c shows the correlation between the attenuation (in dB) and the received optical power (in dBm). As we can see, the received power evaluate linearly, thus we can directly represent BER and EVM as function of the received power. Figure 10.a and 10.b shows these results, for a center frequency of 550 MHz, transmitted gain of -10 dB and a QPSK modulation. Notice that, we made two types of measurements: one series without encoding and the other with LDPC encoding. Indeed, because LDPC is applied on the received bits, we cannot make any correlation between those EVM and BER when using LDPC. Additionally, we can clearly see in figure 10.b that LDPC enhance the performance of our communication by reducing significantly the BER (without influencing the EVM).

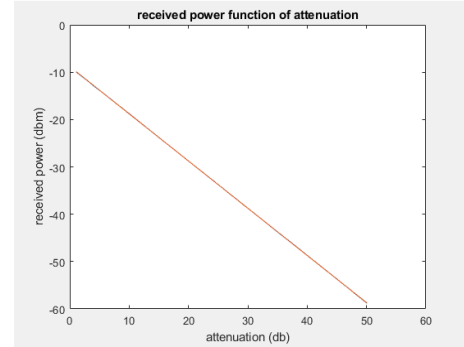


Figure 10.c: evolution of received power function of attenuation.

Relation between EVM and BER.

When using two metrics, it could be useful to see if they are correlated for better interpretation. For that [1][2] propose a method to calculate BER as a function of EVM:

$$P_b = \frac{2(1 - 1/L)}{\text{Log}_2 L} * Q \left[\sqrt{\frac{3 \text{Log}_2 L}{L^2 - 1} \frac{2}{\text{EVR}_{rms}^2 \text{Log}_2 M}} \right] \quad (\text{V.6})$$

Where L is the number of levels in each demodulation (for example L = 2 for QPSK modulation) of a M-ary modulation method (M is the number of points in the constellation). The relation expressed in (V.6) is valid under the assumption that

we are in the case of coherent detection and Gaussian channels. Theoretical and measured BER are represented in figure 11. As we can see, we do not have a perfect correlation between the theoretical curve and the one we obtained. This can be due to different factors from experimental conditions, the main one, that we are using Direct Detection (DD) and not coherent detection. It can be seen in figure 11, that this change means that for the same BER, the DD requires about 2 dB EVR improvement. Which is not too much considering the considerable simplification using DD instead of coherent detection.

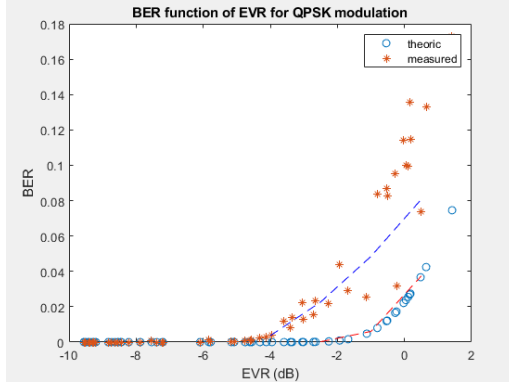


Figure 11: evolution of received power function of attenuation.

D. Future Works

Further works are possible using this communication system. As we mentioned, it could be used for implementing WAVE protocol (because we fulfilled physical layer requirements).

Other Measurements

As we discussed in part V, we did not have enough time material to test our communication system in longer range wireless environments. This is an important problem, considering that it is aimed to be used in vehicles environments. Nevertheless, as shown in figure 10.a/10. b, our system is capable of very good performances, at least for short wireless distances in the range of about 5 centimeters. Nevertheless, checking that wired-wireless-wired transitions have no significant effect. These results are very encouraging to conduct further measurements and performances testing.

WAVE protocol

If someone would like to continue this project, you will find in the appendix a short overview on what is WAVE protocol.

Enhance the Frame detection.

During our measurements, we noticed that our system struggled to find the beginning of the frame (therefore we only reached 30 dB of attenuation instead of continuing). Other techniques than the one proposed by [7] are possible. For example, [16] propose an enhancement of the timing synchronization, based on [7].

VI. CONCLUSION

As we have seen during this report, we have been able to perform wireless optical communication, using IM/DD device, by implementing 802.11p physical layer requirements. We demonstrated that we could use this communication system for V2X application, indeed, our results are very encouraging for further experimentation and enhancement. Even if we have not been able to test our system on a long-range wireless environment, its performances on a attenuated signal are promising for the future of optical communication in vehicle environment. As we mentioned in the introduction, constructors and operators are always seeking new technologies to support the number of equipment implied in V2X. Therefore, this project is a first approach for an interesting alternative to RF domain communications.

VII. APPENDIX

The Wireless Access in Vehicular Environments (WAVE) is part of the 802.11p standard, made for DSRC, that has been validated by the 3GPP organization. standard using the MAC layer to perform ad-hoc communications.

General Process.

In WAVE functionate with two types of channels (see figure 2): A Control Channel (CCH) which is used for basic messages needed for cooperative driving and safety issue. 6 Services Channels (SCH), each one corresponding to a certain type of messages [12].

The access to the one or the other channel is depending on a synchronization time interval of 100ms. During this period, which is composed of one CCH interval, one SCH interval and also two guard band intervals to prevent from interferences caused by possible delays during the transmission (see figure 3). At the beginning of each CCH interval, every transmitter switch to the CCH frequency and can send messages (after authorization, see c)), of course, at the beginning of each SCH interval, transmitter must switch to the SCH frequency.

Type of messages and priorities.

Only three types of messages can be exchange on the CCH:

- short status message (beacons), they are sent periodically to signal the presence of a vehicle to its neighbour, give information about its velocity, position, etc...
- WBBS, used to set-up a future transmission during the SCH.
- WAS to advertise a WBBS.
- Life safety messages, in the situation of an imminent collision for example.

The rest of the messages is sent during the SCH interval on one of the 6 services channels.

Because of the safety issue, some messages are more important than others, for example an imminent collision awareness message is more prior than a beacon.

Therefore, WAVE also implement a system of four priorities on top of the two channels, depending on this priority, the time before sending the message is longer for a message with a lower priority.

Channel access.

A message needs to wait into a buffer before being sent, the selection process is in two phases. First, the messages will content internally, a waiting time is fixed depending of the priority $t_a = AIFS * t_s$ with t_a the time before being selected, $t_s = 16$ s is the time slot and AIFS stand for Arbitrary Interframe Space fixed by the standard. After this phase, the transmitter will start the transmission only if it detects the channel in idle mode (free of transmission) for a time equal to AIFS seconds. If the channel is not free when the message is ready for transmission, a random number called the contention window (CW) is picked randomly between 0 and CWmin. Every time the transmitter detects an idle time in the channel, this number is decremented, when CW reach 0, the transmission can start. The lowest priority has the higher value of CWmin. In case of collision, the transmission will be retried but this time, instead of detecting AIFS seconds of idle mode, the standard uses the Extended Interframe Space (EIFS).

A. EVM for BPSK modulation

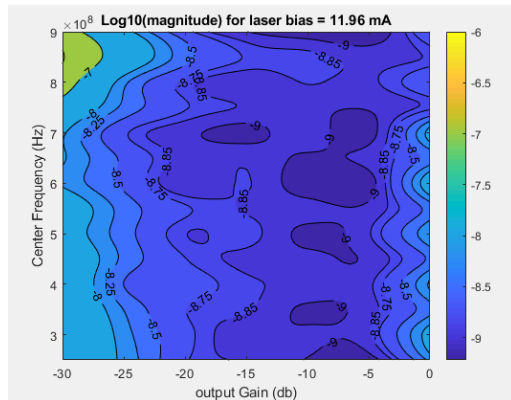


Figure 12.a: evolution of EVM, function of center frequency and output gain. Representation using $10 * \text{Log}_{10}(\text{EVM})$ for BPSK.

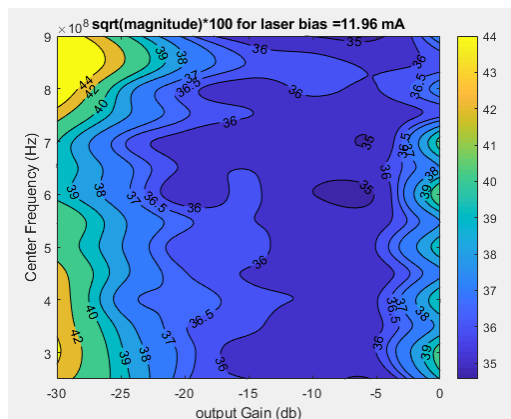


Figure 12.b: evolution of EVM, function of center frequency and output gain. Representation using $\text{sqrt}(\text{EVM}) * 100$ (percentage) for BPSK.

VIII. REFERENCE

- [1]: *On the extended relationships among EVM, BER and SNR as performance metrics*, Shafik, Rishad Ahmed and Rahman, Md Shahriar and Islam, AHM Razibul, 2006 International Conference on Electrical and Computer Engineering, Pages 408-411, 2006, IEEE.
- [2]: *On the error vector magnitude as a performance metric and comparative analysis*, Shafik, Rishad Ahmed and Rahman, Md Shahriar and Islam, AHM Razibul and Ashraf, Nabil Shovon, 2006 International Conference on Emerging Technologies, Pages 27-31, 2006, IEEE.
- [4]: *Direct detection analog optical links*, Cox, Charles and Ackerman, Edward and Helkey, Roger and Betts, Gary E, IEEE Transactions on Microwave theory and techniques, Volume 45, Number 8, Pages 1375-1383, 1997, IEEE.
- [5]: Jack Keil Wolf, Spring 2010, *An Introduction to Error correction code, Part 3*, [online], available at: <file:///D:/Users/Documents/upc/sujet%20recherche/article%20for%20report/ErrrorCorrectionIII.pdf>.
- [6]: *Performance analysis and complexity study of LDPC and turbo coding schemes for inter vehicle communications*, Kiokes, George and Economakos, George and Amditis, Angelos and Uzunoglu, Nikolaos K, 2011 11th International Conference on ITS Telecommunications, Pages 559-564, 2011, IEEE.
- [7]: *Robust frequency and timing synchronization for OFDM*, Schmidl, Timothy M and Cox, Donald C, IEEE transactions on communications, Volume 45, Number 12, Pages 1613-1621, 1997, IEEE.
- [8]: *Pseudo noise sequences for engineers*, Mutagi, RN, Electronics & communication engineering journal, Volume 8, Number 2, Pages 79-87, 1996, IET.
- [9]: *The physical layer of the IEEE 802.11 p WAVE communication standard: the specifications and challenges*, Abdelgader, Abdeldime MS and Lenan, Wu, Proceedings of the world congress on engineering and computer science, Volume 2, Pages 22--24, 2014.
- [10]: *3GPP LTE versus IEEE 802.11 p/WAVE: Which technology is able to support cooperative vehicular safety applications?*, Vinel, Alexey, IEEE Wireless Communications Letters, Volume 1, Number 2, Pages 125--128, 2012, IEEE.
- [11]: *Use cases, requirements, and design considerations for 5G V2X*, Boban, Mate and Kousaridas, Apostolos and Manolakis, Konstantinos and Eichinger, Joseph and Xu, Wen, arXiv preprint arXiv:1712.01754, 2017.
- [12]: *Performance evaluation of the IEEE 802.11 p WAVE communication standard*, Eichler, Stephan, 2007 IEEE 66th Vehicular Technology Conference, Pages 2199-2203, 2007, IEEE.
- [13]: *On the performance of different OFDM based optical wireless communication systems*, Mesleh, Raed and Elgala, Hany and Haas, Harald, IEEE/OSA journal of optical communications and networking, Volume 3, Number 8, Pages 620-628, 2011, IEEE.
- [14]: *IEEE 802.11 p Ahead of LTE-V2V for Safety Applications*, Filippi, Alessio and Moerman, Kees and Martinez, Vincent and Turley, Andrew and Haran, Onn and Toledano, Ron, Autotalks NXP, 2017.
- [15]: MathWorks Team, *OFDM synchronization*, [Online], available at : <https://uk.mathworks.com/help/comm/examples/ofdm-synchronization.html>
- [16]: *A robust timing and frequency synchronization for OFDM systems*, Minn, Hlaing and Bhargava, Vijay K and Letaief, Khaled Ben, IEEE transactions on wireless communications, Volume 2, Number 4, Pages 822-839, Year 2003, IEEE.
- [17]: *On the generator matrix of array LDPC codes*, Baldi, Marco and Bianchi, Marco and Cancellieri, Giovanni and Chiaraluce, Franco and Klove,

Torleiv, SoftCOM 2012, 20th International Conference on Software, Telecommunications and Computer Networks, Pages 1-5, 2012, IEEE

[18] : ADALM-PLUTO Radio Support from Communications Toolbox, [online] available at : <https://uk.mathworks.com/hardware-support/adalm-pluto-radio.html>